Photoluminescence of Zn Se x Te 1 x Zn Te multiple-quantum-well structures grown by molecular-beam epitaxy

Y. T. Shih, Y. L. Tsai, C. T. Yuan, C. Y. Chen, C. S. Yang, and W. C. Chou

Citation: Journal of Applied Physics **96**, 7267 (2004); doi: 10.1063/1.1818712
View online: http://dx.doi.org/10.1063/1.1818712
View Table of Contents: http://scitation.aip.org/content/aip/journal/jap/96/12?ver=pdfcov
Published by the AIP Publishing

Photoluminescence of $ZnSe_xTe_{1-x}$/ZnTe multiple-quantum-well structures grown by molecular-beam epitaxy

Y. T. Shih[a)]
Institute of Photonics, National Changhua University of Education, Changhua, Taiwan 50007, Republic of China

Y. L. Tsai
Institute of Applied Physics, Chung Yuan Christian University, Chungli, Taiwan 32023, Republic of China

C. T. Yuan, C. Y. Chen, C. S. Yang, and W. C. Chou
Institute of Electrophysics, National Chiao Tung University, Hsinchu, Taiwan 30050, Republic of China

(Received 21 May 2004; accepted 23 September 2004)

This work investigates photoluminescence (PL) spectra from $ZnSe_xTe_{1-x}$/ZnTe multiple-quantum-well structures grown on GaAs(001) substrates by molecular-beam epitaxy. The PL data reveal that the band alignment of the $ZnSe_xTe_{1-x}$/ZnTe system is type II. The thermal activation energy for quenching the PL intensity was determined from the temperature-dependent PL spectra. The activation energy was found to increase initially and then decrease as the thickness of the $ZnSe_xTe_{1-x}$ layers decreases from 7 to 3 nm. The temperature-dependent broadening of the PL linewidth was also investigated. The LO-phonon scattering was found to be the dominant broadening mechanism. © *2004 American Institute of Physics*. [DOI: 10.1063/1.1818712]

I. INTRODUCTION

The wide-band-gap II-VI semiconductors ZnSe and ZnTe and their mixed crystals $ZnSe_xTe_{1-x}$ have attracted much interest because of their great potential for use as possible blue/green light-emitter materials. During the past several years, remarkable advances in molecular-beam epitaxy (MBE) have enabled the growth of $ZnSe_xTe_{1-x}$ epilayers and $ZnSe_xTe_{1-x}$/ZnTe heterostructures. Many efforts have been made to characterize these structures optically. Brasil and co-workers[1,2] reported the optical characterization of $ZnSe_xTe_{1-x}$ epilayers grown by MBE. Rajakarunanayake and co-workers[3,4] investigated the photoluminescence (PL) spectra from $ZnSe_xTe_{1-x}$/ZnTe superlattices. They found a type-II band alignment with a large valence-band offset. Yang *et al.*[5] investigated the PL spectra from $ZnSe_xTe_{1-x}$ epilayers. The peaks of the Te-bound excitons and excitons bound to the Te clusters have been identified. Baranovskii *et al.*[6] investigated the PL spectra from $ZnSe_xTe_{1-x}$/ZnTe single-quantum wells. The dominant line broadening mechanism was attributed to the compositional disorder. On the other hand, a high-brightness green light-emitting diode, using ZnSeTe as the active layer, has been reported for the realization of blue/green light-emitting devices.[7]

In this work, $ZnSe_xTe_{1-x}$/ZnTe multiple-quantum-well (MQW) structures were grown by molecular-beam epitaxy on GaAs(001) substrates. PL was measured to characterize the structures. The thermal activation energy was determined from the temperature-dependent PL spectra. The variation of the activation energy with the thickness of $ZnSe_xTe_{1-x}$ layers and the temperature-dependent broadening of the PL linewidths were investigated.

[a)]Author to whom correspondence should be addressed; electronic mail: ytshih@cc.ncue.edu.tw

II. EXPERIMENTS

$ZnSe_xTe_{1-x}$/ZnTe ($x=0.22$ and 0.54) MQW structures were grown on GaAs(001) substrates, using a Veeco Applied EPI 620 MBE system. The GaAs substrates were indium mounted on a molybdenum block. Oxides on the surfaces of the substrates were removed by heating the substrates to 650 °C until clear reflection high-energy electron diffraction patterns were observed. Veeco Applied EPI 40 cc low-temperature effusion cells were employed to evaporate the elemental solid sources Zn, Se, and Te. Before the $ZnSe_xTe_{1-x}$/ZnTe multiple-quantum wells were grown, a ZnSe layer of 76 Å for samples A–C ($x=0.54$) and D–F ($x=0.22$) or 2 μm for samples G–I ($x=0.22$), and a ZnTe layer of 360 nm were grown as buffer layers. The ZnSe epilayer was grown as a buffer layer because a recent report[8] demonstrated that the crystallinity of a ZnTe epilayer grown on a GaAs substrate can be remarkably improved using a ZnSe buffer layer, and that the strain of a ZnTe layer with a ZnSe buffer layer was less than that without a ZnSe buffer layer.

During the growth of the $ZnSe_{0.54}Te_{0.46}$/ZnTe ($ZnSe_{0.22}Te_{0.78}$/ZnTe) multiple-quantum wells, the cell temperatures of Zn, Te, and Se were 270 (300), 300 (325), and 155 (160) °C, respectively, while the temperature of the substrate was fixed at 300 °C. Ten periods of $ZnSe_xTe_{1-x}$/ZnTe quantum wells were grown in each sample. The thickness of the ZnTe layers was fixed at 200 Å, whereas the thickness of the $ZnSe_xTe_{1-x}$ layers varied from 30 to 70 Å. After the ten periods of the $ZnSe_xTe_{1-x}$/ZnTe quantum wells had been deposited, a ZnTe layer of 300 Å was grown as a cap layer. The thicknesses of the epilayers were estimated from the growth rate. Energy dispersive x-ray spectroscopy was employed to determine the Se concentration, x, in the $ZnSe_xTe_{1-x}$ epilayers. Table I presents relevant sample parameters.

TABLE I. Sample parameters of $ZnSe_xTe_{1-x}/ZnTe$ multiple-well structures.

Sample	Se concentration x of $ZnSe_xTe_{1-x}$ layers	Thickness of buffer layer ZnSe/ZnTe (nm)	Thickness of layers $ZnSe_xTe_{1-x}/ZnTe$ (nm)
A	0.54	7.6/360	7/20
B	0.54	7.6/360	5/20
C	0.54	7.6/360	3/20
D	0.22	7.6/360	7/20
E	0.22	7.6/360	5/20
F	0.22	7.6/360	3/20
G	0.22	2000/360	7/20
H	0.22	2000/360	5/20
I	0.22	2000/360	3/20

Photoluminescence was measured to characterize the samples optically. The samples were loaded onto the cold finger of a closed-cycle refrigerator to maintain their temperatures from 10 to 300 K. A 351.0-nm beam at an average power of 10 mW from an argon-ion laser was used to excite the PL spectra. A SPEX 1403 double-grating spectrometer, equipped with a thermoelectric-cooled photomultiplier tube, was employed to analyze the spectra.

III. RESULTS AND DISCUSSION

Figure 1 presents the low-temperature PL spectra obtained from $ZnSe_xTe_{1-x}/ZnTe$ MQW structures. These PL spectra include two types of emission peaks. As the thickness of the $ZnSe_xTe_{1-x}$ layers decreases, the emission peaks at higher energies (labeled E_X) exhibit a large blueshift, while those at lower energies (labeled E_D) remain in the same position. The E_X emission peaks are associated with the interband excitonic transition. The composition-dependent energy gap of the MBE-grown $ZnSe_xTe_{1-x}$ epilayers at the low temperature can be expressed as[1]

$$E_g(x) = xE_{\mathrm{ZnSe}} + (1-x)E_{\mathrm{ZnTe}} - bx(1-x), \quad (1)$$

where $E_{\mathrm{ZnSe}}=2.820$ eV and $E_{\mathrm{ZnTe}}=2.392$ eV are the energy-band gaps for ZnSe and ZnTe, respectively, and $b=1.507$ eV is the bowing parameter. Accordingly, the emission energies of the E_X peaks in Fig. 1 are less than the energy gaps of either ZnTe or $ZnSe_xTe_{1-x}$. This result reveals that the E_X transitions in Fig. 1 are type-II transitions. Figure 2 schematically depicts the band alignment of the $ZnSe_xTe_{1-x}/ZnTe$ system. In this type-II system, electrons are confined in the $ZnSe_xTe_{1-x}$ layers while holes are confined in the ZnTe layers. Therefore, the lowest energy interband transition (labeled E_X) is spatially indirect. The large blueshift of the E_X emission peaks is attributed to the quantum confinement of electrons. As the thickness of the $ZnSe_xTe_{1-x}$ layers decreases, the strong quantum confinement increases the subband energy E_e in the $ZnSe_xTe_{1-x}$ quantum well and increases the interband transition energies.

The E_D emission peaks in Fig. 1 do not shift as the thickness of the $ZnSe_xTe_{1-x}$ layers decreases and so can be assigned to optical transitions related to interface defects. PL measurements were made for samples G–I to examine the origin of the E_D peaks. Figure 3 presents the results. The

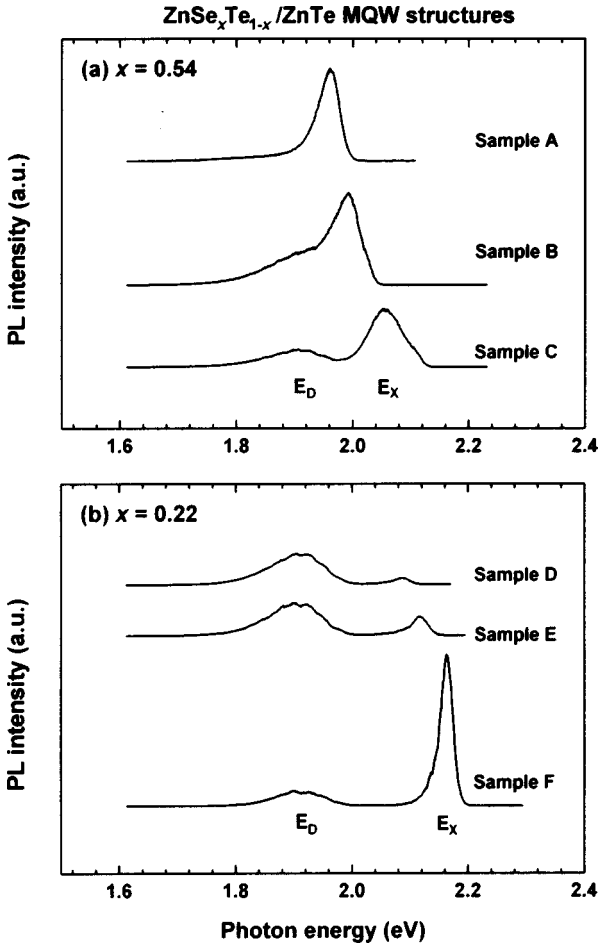

FIG. 1. Photoluminescence spectra of $ZnSe_xTe_{1-x}/ZnTe$ multiple-quantum-well structures.

growth parameters of samples G–I were similar to those of samples D–F, except that the buffer layers of samples G–I were thicker. The thicker buffer layers reduce the effect of the interface defects on the PL spectra. Therefore, Fig. 3 does not exhibit the E_D peaks.

The temperature dependence of the PL spectra was also investigated. Figure 4(a) presents the temperature-dependent PL spectra from sample C. The temperature dependence

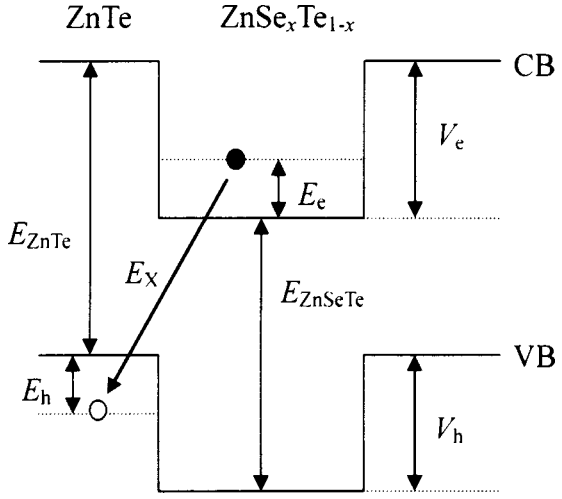

FIG. 2. Band alignment of $ZnSe_xTe_{1-x}/ZnTe$ system.

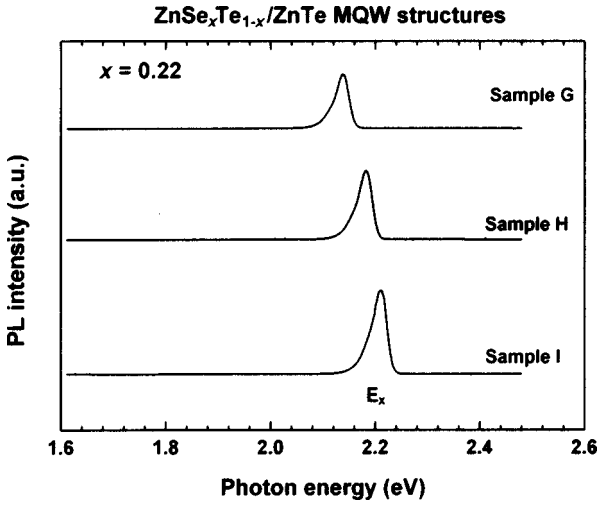

FIG. 3. Photoluminescence spectra of samples G–I of $ZnSe_xTe_{1-x}/ZnTe$ multiple-quantum-well structures.

from the PL spectra of the other samples reveals similar optical characteristics. As the temperature increases, the PL intensity drops rapidly and the interband exciton transition peaks are redshifted and broadened. The redshift is caused by the decrease in the band-gap energy as the temperature increases. Additionally, the small binding energy of the exciton in a type-II band alignment system is such that at higher temperature, the thermal energy is comparable to the binding energy of the exciton, and the exciton-phonon interaction is considerable, resulting in a weaker and broader PL peak.

The temperature dependence of the integrated PL intensity (I_{PL}) of an exciton emission peak could be expressed as[9,10]

$$I_{PL}(T) = \frac{I_0}{1 + A \exp(-E_A/k_B T)}, \tag{2}$$

where T is the temperature, k_B is the Boltzmann constant, I_0 is the integrated PL intensity near 0 K, A is a constant, and E_A is the thermal activation energy. E_A is responsible for the quenching of PL intensity in the temperature-dependent PL spectra. Figure 4(b) presents the measured I_{PL} for sample C as a function of temperature. As the temperature increases to 50–60 K, an abrupt drop of over one order of magnitude in the integrated PL intensity is observed. These measured values of integrated PL intensity were fitted using Eq. (2) and the thermal activation energy E_A of the MQW structures was obtained. Usually, E_A is obtained simply from the slope of the Arrhenius plot of $\ln(I_{PL})$ versus $1/T$ at the high-temperature limit. However, such a method might cause a large error because it relies entirely on data measured at high temperature. Figure 4(b) clearly shows that the theoretical curve is satisfactorily consistent with the experimental data. Similar results were obtained for the other samples.

Figure 5 presents the obtained thermal activation energies E_A of samples A–C ($x=0.54$) and D–F ($x=0.22$). E_A is plotted as a function of the thickness of the $ZnSe_xTe_{1-x}$ layers. The thickness of the $ZnSe_xTe_{1-x}$ layers decreases from 7 to 3 nm, and E_A tends to increase initially and then decrease.

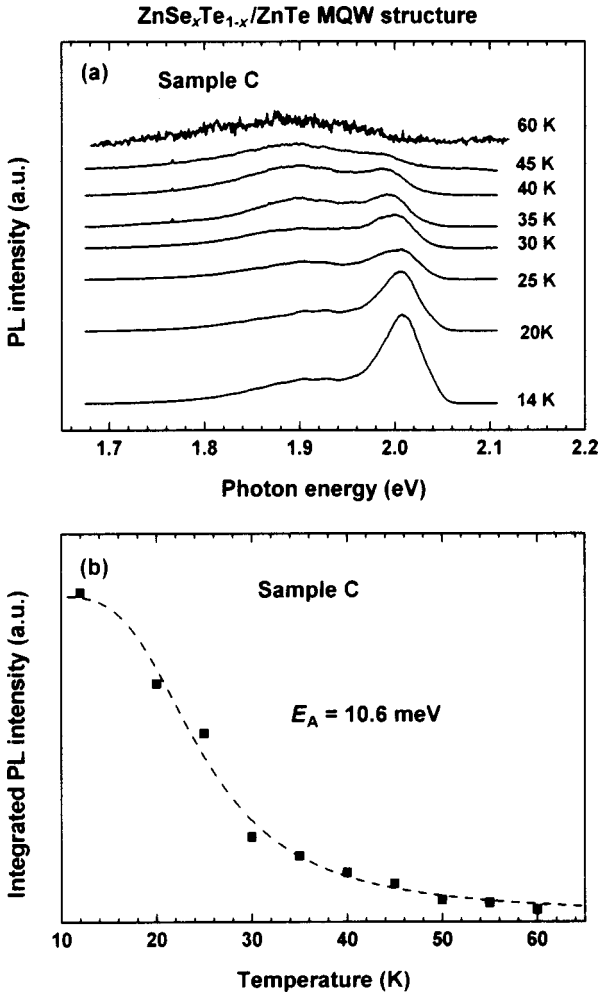

FIG. 4. (a) Temperature-dependent photoluminescence spectra of sample C of $ZnSe_xTe_{1-x}/ZnTe$ multiple-quantum-well structures. (b) Variation of integrated PL intensity with temperature of sample C of $ZnSe_xTe_{1-x}/ZnTe$ multiple-quantum-well structures.

The temperature-induced quenching of luminescence in the MQW structures proceeds mainly by two mechanisms: thermal emission of (at least one type of) charge carriers out of confined quantum-well states into barrier states[11] and thermal dissociation of excitons into free-electron-hole pairs.[10] Electrons are confined in $ZnSe_xTe_{1-x}$ layers, whereas holes are confined in ZnTe layers so samples with wider $ZnSe_xTe_{1-x}$ layers exhibit weaker wave-function overlap, which results in small exciton binding energy. Therefore, the second quenching mechanism dominates. The primary means of quenching PL intensity is the thermal dissociation of excitons into free-electron-hole pairs. After the excitons have been broken apart, electrons are free to diffuse into the barrier, and the PL is quenched. The thermal activation energy E_A for this process is determined from the exciton binding energy and decreases as the thickness of the $ZnSe_xTe_{1-x}$ layers increases.

However, samples with narrower $ZnSe_xTe_{1-x}$ layers have narrower wells and therefore increased subband energy E_c of the electrons (Fig. 2). The structures herein are common-cation systems, so the conduction-band offset is small and leads to small delocalization energy $V_e - E_c$, facilitating the escape of the electrons from the quantum wells. Therefore,

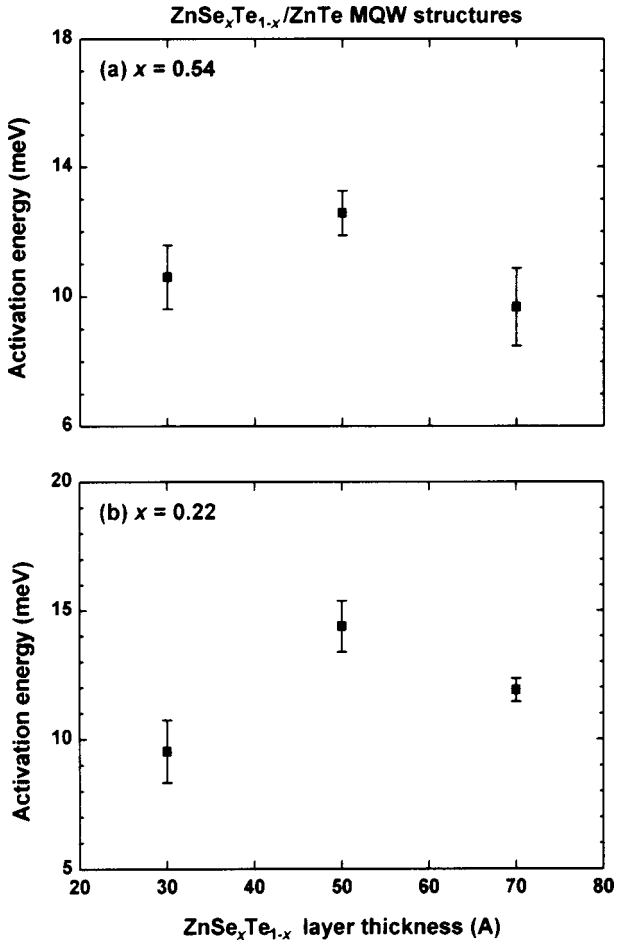

FIG. 5. Variation of activation energy with thickness of $ZnSe_xTe_{1-x}$ layers in $ZnSe_xTe_{1-x}$/ZnTe multiple-quantum-well structures.

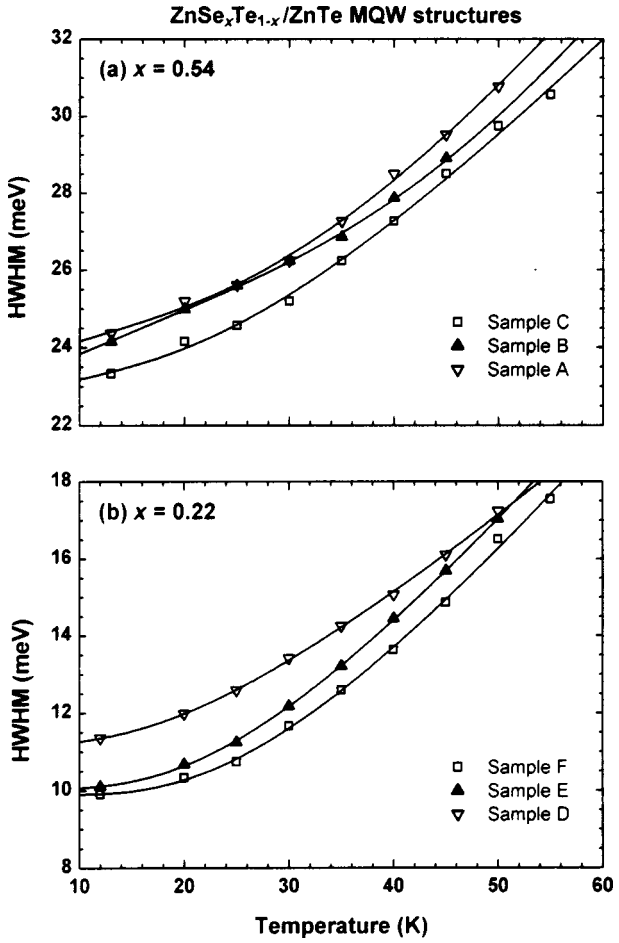

FIG. 6. Variation of PL linewidth with temperature of $ZnSe_xTe_{1-x}$/ZnTe multiple-quantum-well structures.

the first quenching mechanism dominates. The main cause of the quenching of the PL intensity is the thermal emission of electrons into barrier states. The activation energy E_A can be regarded as the delocalization energy of electrons and decreases as the thickness of the $ZnSe_xTe_{1-x}$ layers decreases.

The temperature-dependent broadening of exciton emission peaks of the $ZnSe_xTe_{1-x}$/ZnTe MQW structures was also investigated. Figure 6 presents the linewidths [half width at half maximum (HWHM)] of the PL peaks as functions of temperature. The luminescence linewidths gradually increase with temperature. Scattering processes with acoustic phonons, LO phonons, and ionized impurities are considered, and the temperature-dependent luminescence linewidth of excitons in quantum wells thus expressed as[12]

$$\Gamma(T) = \Gamma_0 + \Gamma_{\mathrm{LA}} T + \frac{\Gamma_{\mathrm{LO}}}{\exp(\hbar\omega_{\mathrm{LO}}/k_B T) + 1} + \Gamma_{\mathrm{imp}} \exp(-\langle E_b \rangle / k_B T), \quad (3)$$

where Γ_0 is the inhomogeneous broadening, Γ_{LA} is the coefficient of the exciton–acoustic-phonon interaction, Γ_{LO} is the exciton–LO-phonon coupling constant, $\hbar\omega_{\mathrm{LO}}$ is the LO-phonon energy, Γ_{imp} is a factor of proportionality that accounts for the density of the impurities, and $\langle E_b \rangle$ is the impurity binding energy averaged over all possible locations of the impurities.

The measured PL linewidths were fitted by Eq. (3). The solid curves in Fig. 6 represent the theoretical results. They agree well with the experimental data. Table II presents the fitted values of Γ_0, Γ_{LA}, Γ_{LO}, and $\hbar\omega_{\mathrm{LO}}$. In the fitting procedure, the contribution of the impurity scattering process to linewidth broadening can be ignored, so $\Gamma_{\mathrm{imp}}=0$. Therefore, the concentrations of impurities in the samples herein were very low. Figure 6 and Table II together reveal that LO-phonon scattering is the mechanism that dominates the broadening of the linewidth as the temperature increases.

TABLE II. Parameters obtained by fitting Eq. (3) to the HWHM VS T data in Fig. 6.

	Parameters			
Sample	Γ_0 (meV)	Γ_{LA} (10−2 meV/K)	Γ_{LO} (meV)	$\hbar\omega_{\mathrm{LO}}$ (meV)
A	23.37	8.02	38.56	10.80
B	22.71	11.27	86.06	17.08
C	22.59	6.01	22.92	8.27
D	10.94	3.23	15.21	6.29
E	9.91	1.47	27.46	7.18
F	9.88	0.18	31.61	7.73

IV. SUMMARY

In summary, $ZnSe_xTe_{1-x}/ZnTe$ ($x=0.22$ and 0.54) multiple-quantum-well structures were grown on GaAs(001) substrates using a Veeco Applied EPI 620 molecular-beam epitaxy system. Photoluminescence spectra were measured to characterize optically the MQW structures. The emission peaks from the interband transition were blueshifted as the thickness of the $ZnSe_xTe_{1-x}$ layers decreased. The PL data reveal that the band alignment of $ZnSe_xTe_{1-x}/ZnTe$ system is type II.

The temperature dependence of the PL spectra was investigated. As the temperature increased, the PL peaks became weaker and broader. The thermal activation energy that is responsible for quenching the PL intensity was determined from the plots of integrated PL intensity versus temperature. The activation energy tended to increase initially and then decrease as the thickness of the $ZnSe_xTe_{1-x}$ layers decreased from 7 to 3 nm. For samples with wider $ZnSe_xTe_{1-x}$ layers, the primary mechanism of quenching the PL intensity is thermal dissociation of excitons into free-electron-hole pairs. For samples with narrower $ZnSe_xTe_{1-x}$ layers, the dominant quenching mechanism is thermal emission of electrons into barrier states. The temperature-dependent broadening of PL linewidth was analyzed in terms of exciton–acoustic-phonon and exciton–LO-phonon scattering processes. LO-phonon scattering was found to be the dominant broadening mechanism.

ACKNOWLEDGMENT

The authors would like to thank the National Science Council of the Republic of China for financially supporting this research under Contract Nos. NSC-92-2112-M-018-014, NSC-93-2112-M-018-005, and NSC-92-2112-M-009-041.

[1] M. J. S. P. Brasil, R. E. Nahory, F. S. Turco-Sandroff, H. L. Gilchrist, and R. J. Martin, Appl. Phys. Lett. **58**, 2509 (1991).
[2] F. S. Turco-Sandroff, R. E. Nahory, M. J. S. P. Brasil, R. J. Martin, and H. L. Gilchrist, Appl. Phys. Lett. **58**, 1611 (1991).
[3] Y. Rajakarunanayake, M. C. Phillips, J. O. McCaldin, D. H. Chow, D. A. Collins, and T. C. McGill, Proc. SPIE **1285**, 142 (1990).
[4] M. C. Phillips, Y. Rajakarunanayake, J. O. McCaldin, D. H. Chow, D. A. Collins, and T. C. McGill, Proc. SPIE **1285**, 152 (1990).
[5] C. S. Yang, D. Y. Hong, C. Y. Lin, W. C. Chou, C. S. Ro, W. Y. Uen, W. H. Lan, and S. L. Tu, J. Appl. Phys. **83**, 2555 (1998).
[6] S. D. Baranovskii, U. Doerr, P. Thomas, A. Naumov, and W. Gebhardt, Phys. Rev. B **48**, 17149 (1993).
[7] D. B. Eason *et al.*, Appl. Phys. Lett. **66**, 115 (1995).
[8] T. W. Kim and H. I. Lee, Mater. Res. Bull. **37**, 1763 (2002).
[9] J. D. Lambkin, D. J. Dunstan, K. P. Homewood, L. K. Howard, and M. T. Emeny, Appl. Phys. Lett. **57**, 1986 (1990).
[10] I. Y. Gerlovin, Y. K. Dolgikh, V. V. Ovsyankin, Y. P. Efimov, I. V. Ignat'ev, and E. E. Novitskaya, Phys. Solid State **40**, 1041 (1998).
[11] S. Weber, W. Limmer, K. Thonke, R. Sauer, K. Panzlaff, G. Bacher, H. P. Meier, and P. Roentgen, Phys. Rev. B **52**, 14739 (1995).
[12] J. Lee, E. S. Koteles, and M. O. Vassell, Phys. Rev. B **33**, 5512 (1986).